ACS APPLIED MATERIALS & INTERFACES

RESEARCH ARTICLE

www.acsami.org

Stress Delocalization in Crack Tolerant Electrospun Nanofiber Networks

Urszula Stachewicz,[†] Ilker Peker,[‡] Wei Tu,[†] and Asa H. Barber[*,‡]

[†]Nanoforce Technology, Ltd. and [‡]Department of Materials, School of Engineering and Materials Science, Queen Mary University of London. Mile End Road, London E1 4NS, United Kingdom

ABSTRACT: The fracture toughness of a noncontinuum fibrous network produced by electrospinning polyamide 6 nanofibers is investigated. The mechanical properties of the nanofiber network is observed to be independent of various incorporated macroscopic crack lengths, resulting in an apparent increase in fracture toughness with increasing crack length as evaluated using conventional fracture mechanics. Strain mapping of the nanofiber network indicates stress delocalization mechanisms operating around these macroscopic cracks in the network. The deformation behavior of the nanofiber network will therefore depend on the volume of fibers being loaded in the network and not the number of fibers in the cross-sectional width defining continuum sample mechanics. These results indicate a propensity for both the synthetic electrospun nanofibrous network in this work and potentially other nanofibrous networks to resist failure from macroscopic cracks incorporated within the material.

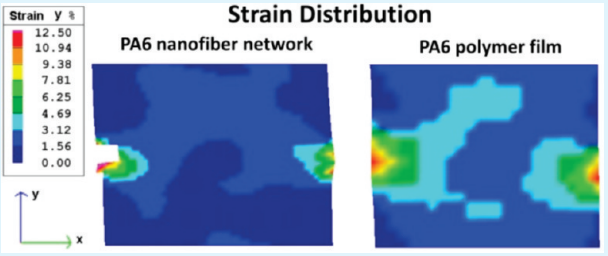

KEYWORDS: electrospinning, stress delocalization, mechanics, fiber networks

INTRODUCTION

Tough materials are required in applications where crack propagation needs to be suppressed or controlled to avoid ultimate material failure. The propagation of a crack occurs when the local stress concentration at the crack tip causes material failure ahead of the crack. A number of biological and biomimetic structures have enhanced their overall material toughness by promoting crack deflection mechanisms locally within the material, typically using layered structures.[1] For example, bone material, depending on the function and location, exhibits a fiber laminate structure with variable fiber orientation and mineral content to prevent the propagation of microcracks through the sample thickness by crack deflection between the laminate sheets.[2] The same principle of laminate and layered structures is extensively used for introducing toughness in synthetic composite materials[3] and unique crystal structures around fiber reinforcements in polymer composites have exhibited layered, or "treeing", type failure for enhanced toughness through stress delocalization around crack tips.[4] Rubbery particulates incorporated within intrinsically brittle solid polymers are an additional common method of increasing toughness. Rubbery particles within a polymer reduces plastic resistance of the composite as the debonding stress takes place between particles and polymer matrix, creating precavitated material during stretching and consequently providing toughening by crack tip shielding.[5] Composites with embedded steel chains in a polymer matrix show lock-up mechanisms by transferring load between interlocks and preventing local deformation.[6] While a number of these biological and synthetic materials are effectively fiber composites, structures formed of noncontinum fibrous networks are commonly used in a number of applications such as packaging or protective clothing industry where crack propagation needs to be restricted. Interestingly, nature has exploited fibrous networks for functions where critical failure of the network through crack propagation is undesirable. One particular example is spider's web, which is constructed of natural polymeric silk fibers and used as a network in order to trap the prey of the spider.[7] Catastrophic failure of the web network must be avoided through tolerance to macroscopic cracks in the web to maintain function.[8] While the silk fibrous material has been studied extensively and found to possess considerable toughness because of high fiber failure strain[9] and nanofibril structural features that restrict crack propagation within the silk fiber itself,[10] less is known about the mechanical behavior of the network. Other natural fibrous networks with a prominent mechanical function include bacterial cellulose,[11] extra-cellular matrix sheets,[12] and actin networks.[13] Critically, the network integrity is paramount in achieving mechanical function in these fibrous networks, indicating a propensity for the network to be tough. The importance of fibrous networks in nature has led to considerable theoretical descriptions of these networks by accounting for both the mechanical properties of the individual fiber elements[14] as well as frictional behavior and interactions between fibers.[15] Typically these theoretical descriptions account for the nanofibrous geometries found in such biological networks. Analytical modeling of fibrous networks has indicated how interfiber interactions can cause significant energy dissipation through plastic deformation, essentially fiber−fiber sliding, over a diffuse network volume before ultimate failure of the

Received: February 26, 2011
Accepted: May 5, 2011
Published: May 05, 2011

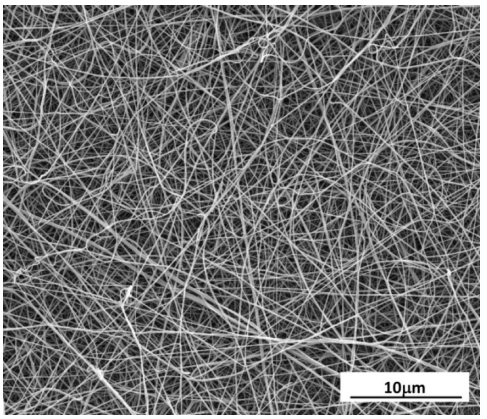

Figure 1. Electron micrograph highlighting the nonwoven network of electrospun PA6 nanofibers.

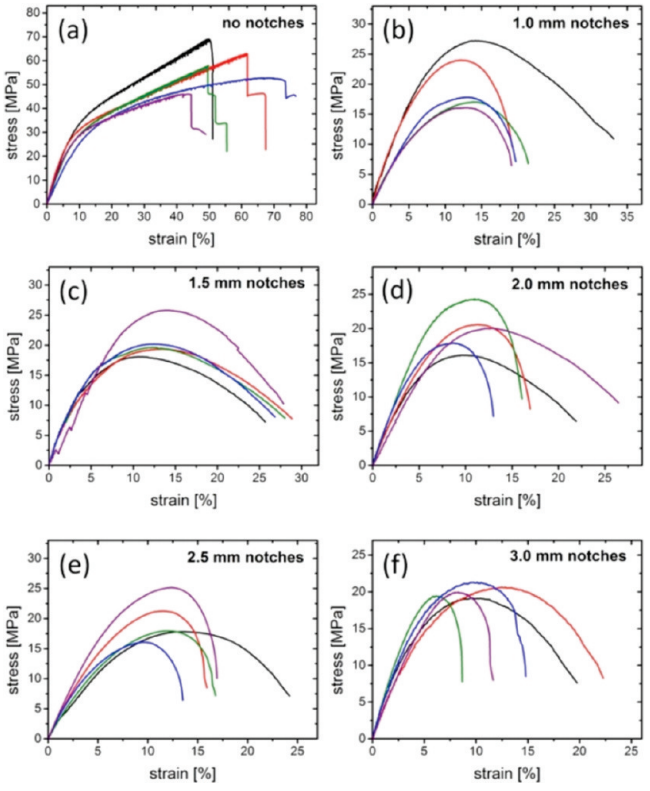

Figure 2. Stress−strain curves obtained from tensile tests on electrospun PA6 nanofiber samples (a) without notches and with (b) 1 mm, (c) 1.5 mm, (d) 2 mm, (e) 2.5 mm, and (f) 3 mm double-edge notches.

material.[16] Modification of these interfiber interactions has been addition shown theoretically to increase the strength and toughness of the nanofiber network.[17] However, manufactured nanofibrous materials have yet to exploit the potential toughening mechanisms of these network systems.

Electrospinning is perhaps the most common method for producing nonwoven polymeric material synthetically that closely resembles biological material counterparts as shown in Figure 1.[18] Electrospun polymer fibers can be fabricated from a range of polymer precursors, with the fiber diameter,[19] porosity of the resultant fibrous network[20] controllable by changing spinning

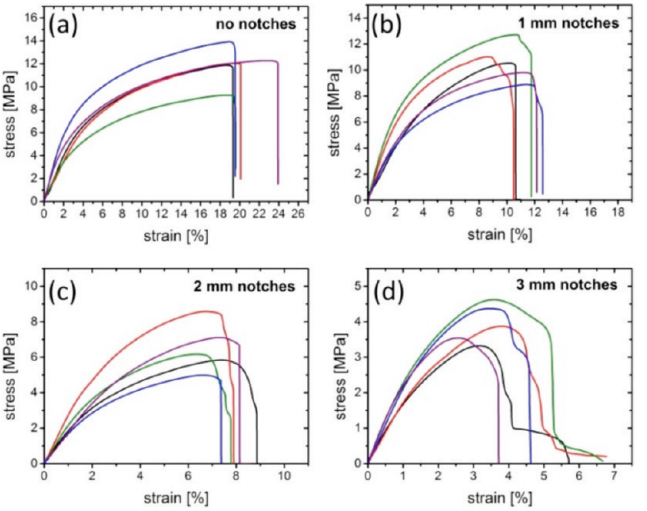

Figure 3. Stress−strain curves obtained from tensile tests on PA6 film samples (a) without notches and with (b) 1 mm, (c) 2 mm, and (d) 3 mm double-edge notches.

parameters,[21] in addition to fiber organization tailored through the use of patterned electrodes or rotating collectors.[22] As the porosity of polymers has shown to be effective in increasing toughness in a similar way to natural materials,[23] electrospun polymer fiber networks may exhibit an inherent resistance to fracture.

The mechanical properties of electrospun polymer fibers have been examined using techniques including string pendulum principles for fibers with attached mass,[24] indentation,[25,26] bending,[27] and tensile testing using atomic force microscopy (AFM).[28] The mechanical properties of electrospun fibers are generally seen to exhibit size dependent effects, with smaller diameter electrospun nanofibers possessing a higher elastic modulus.[29] In addition, recent work has shown how electrospun fiber surfaces show higher surface free energies when compared to bulk polymer materials.[30] Thus, electrospun nanofibrous networks may exhibit distinct behavior when compared to bulk equivalents. As with biological fibrous networks, studies of electrospun fibrous networks and their mechanisms of deformation has been less well investigated, although notably the optimized elastic properties of electrospun fibrous networks have been shown to be critical in improving cell adhesion and protein absorption interactions in tissue engineering scaffolds.[31] However, the fracture toughness of electrospun fibrous polymer networks are generally poorly understood and may also provide a model system in describing mechanical behavior of other biologically produced networks such as spider web. The aim of this work is therefore to examine the mechanical properties of electrospun fibrous polymer networks to investigate potential toughening mechanisms.

MATERIALS AND METHODS

Materials. Polyamide 6 (PA6, BASF, Ultramid B33 L, Germany) was dissolved in a mixture of acetic acid (≥99.7%, Sigma Aldrich, U.S.A.) and formic acid (98%, Sigma Aldrich, U.S.A.) (50/50 mass ratio) to produce a resultant polymer concentration of 12 wt.% in solution. The PA6 polymer solution was electrospun into nanofibers using a large scale multijet electrospinning setup (NanoSpider, Elmarco, Czech Republic). A voltage of 55 kV was applied between a rotating wire cylinder and an aluminum sheet acting as a ground electrode 18 cm above the cylinder. The rotating wires moved through the prepared polymer solution to allow

Table 1. Average Tensile Stress, Tensile Strain, Elastic Modulus, and Fracture Toughness for Electrospun PA6 Fibrous Network and PA6 Film Samples without Notches and with Different Double Edge Notch Lengths

samples	notch length [mm]	average tensile failure stress [MPa]	average tensile strain to failure [%]	average elastic modulus [MPa]	average fracture toughness [MPa $m^{1/2}$]
PA6 fibrous network		57.73 ± 8.93	52.94 ± 12.26	418.46 ± 92.63	
	1.0	20.40 ± 4.92	15.00 ± 4.36	266.06 ± 48.35	1.27 ± 0.31
	1.5	20.60 ± 3.01	12.63 ± 1.37	407.10 ± 90.90	1.59 ± 0.23
	2.0	19.77 ± 3.06	10.62 ± 1.65	307.27 ± 55.89	1.82 ± 0.29
	2.5	19.64 ± 3.60	11.87 ± 1.48	332.42 ± 43.56	2.07 ± 0.39
	3.0	19.74 ± 1.15	9.40 ± 2.36	391.22 ± 57.80	2.64 ± 0.10
PA6 film		11.89 ± 1.69	20.82 ± 1.35	235.17 ± 55.61	
	1.0	10.59 ± 1.43	10.38 ± 1.13	287.08 ± 85.49	0.66 ± 0.09
	2.0	6.54 ± 1.37	6.77 ± 0.55	382.01 ± 115.17	0.60 ± 0.13
	3.0	3.94 ± 0.55	3.30 ± 0.46	212.77 ± 28.38	0.52 ± 0.07

pick-up of solution droplets at the wire surfaces. The applied voltage caused charge build-up at the wire surfaces containing the droplets until cone-jet formation and stretching jets toward the ground electrode occurred at the applied voltage, where nanofibers are deposited.[18,32] The electrospun fiber diameter was 186 ± 3.5 nm as measured using scanning electron microscopy (Inspect F, FEI Company, U.S.A./E.U.). The PA6 solution for electrospinning was subsequently used to prepare comparable continuous PA6 films. The polymer solution was solution cast onto flat aluminum foil and allowed to evaporate at room temperature (20 °C) in a fume cupboard. The film was left to dry for 48 h and removed from the aluminum foil.

Mechanical Testing. Nanofiber network samples were cut from the electrospun mat collected at the aluminum ground electrode with a length and width of 60 mm × 8 mm. The same size samples were cut from cast PA6 film. The cross-sectional area of the fibrous network, required for stress analysis, was calculated by measuring the mass of each sample as well as the density using a gas pycnometer (AccuPyc 1330 He, U.S.A.). The electrospun fibers samples gave an average density ρ_{nf} of 1.2 g/cm^3. The electrospun polymer mesh thickness was determined gravimetrically using the weight of nanofibers samples, m_{nf}, with measured mesh length, L, and width, W. The thickness of the sample was therefore found using $t = m_{nf}/\rho_{nf}WL$. Samples were double-notched with a narrow profile scalpel in the middle of the sample to incorporate cracks into the sample. The crack lengths produced at each notch side was 1, 1.5, 2, 2.5, and 3 mm. Tensile testing of nanofiber and film strips were performed using an Instron Universal Testing Machine (Instron 5566, U.K.) with a cross-head speed of 0.5−2 mm/min and load cell of 1 kN (Instron, U.K.). The mechanical test frame uses a high resolution, noncontacting optical extensometer which consists of camera, light filters and software, in order to give accurate strain measurements and avoid sample slippage. Examples of obtained stress−strain curves for the electrospun fiber mats and cast film are shown in Figure 2 and 3. Image analysis to measure the distribution of strain in the sample was achieved using a comparison tensile test of electrospun fiber network and film with 1 mm crack using two cameras (Schneider Kreuznacht, Germany, 2.8−50 mm lenses) set at an angle of 46° to the sample top surface. Samples were covered with a black spray (Monthana, Shock 9000, Germany), to create a mash of small dots on the surface to verified change of strain during of the samples. Images of the patterned sample surface were taken at 0.1 mm step extensions during tensile testing using the two cameras and analyzed with Aramis software (GOM mbH, version 4.7.4 Germany).

RESULTS AND DISCUSSION

The mechanical properties of the PA6 network as shown in Figure 1 were first examined using tensile testing experiments. The polyamide nanofiber networks provided an average tensile strength of 58 MPa and elastic modulus of 418 MPa, with results summarized in Table 1. Our tensile tests results exhibit higher strength and elastic modulus values when compared to similar mechanical testing experiments[33,34] due to our work accurately measuring the cross-sectional area gravimetrically to account for the network porosity, as defined in the Methods section. The mechanical properties of the electrospun PA6 networks is lower than literature values for individual fibers,[35,36] suggesting fiber sliding as a possible deformation mechanism during tensile testing. The mechanical behavior of a fiber network has been previously examined in terms of fibers sliding from their multi-axial orientation state toward a progressively uniaxial state in the direction of the applied load.[17] Such sliding between nanofibers will produce larger failure strains as progressive alignment of the fibrous elements occurs.[15,16] However, fiber sliding mechanisms will produce poor stress transfer between fibers, resulting in low network tensile strength and elastic modulus.[37,38] Tensile stress−strain behavior of the notched nanofiber network samples, used to characterize how macroscopic cracking propagates within the nanofiber networks in order to examine network toughness, is shown in Figure 2 and Table 1. These representative stress−strain curves highlight how the network samples first exhibit a linear regime, used to determine an elastic modulus, followed by a drop in sample stress with increasing strain until failure. Importantly, we note that the tensile strength and elastic modulus is independent of the crack length. This observation is opposite to PA6 film, where the tensile stress of notched samples decreases with crack notch length as shown in Figure 3 and Table 1. For continuous materials, stress at the crack tip is correlated with a thickness of the sample. A plastic zone is created at the crack tip when a force is applied perpendicular to the crack length. In this zone, material yields and becomes permanently deformed. During the tensile test of thin samples, stresses are distributed and the sample is under so-called plane stress condition.[39] As the nanofiber mats are relatively thin materials, fracture toughness measurements should be based on plain stress conditions. Macroscopically, we can assume that the nanofiber mats are continuous materials with macroscopic cracks. The fracture toughness K_{IC} of the nanofibers mats and film can be calculated as follows:[40]

$$K_{IC} = \sigma_{app} W^{1/2} \left[\tan\left(\frac{\pi a}{W}\right) + 0.1 \sin\left(\frac{2\pi a}{W}\right) \right]^{1/2} \quad (1)$$

where, σ_{app} is maximum stress failure, W is total width of the samples, and a is length of the notched crack.

The variation in the fracture toughness of the fibrous mat calculated from eq 1 with increasing crack length is shown in Figure 4a. A trend is observed where the fracture toughness is apparently increasing with increasing crack length. Such an observation is counterintuitive to typical continuum solids, where the fracture toughness is independent of the notch size.[41] However, the fracture toughness K_{IC} is critically dependent on the width of the sample, which becomes progressively smaller as the crack size increases, thus providing an apparent increase in values of K_{IC} with increasing crack length. Practically, the force required to fail the electrospun mat is independent of the crack length, which is counter to deformation of the film, where K_{IC} is, within error, independent of crack length as shown in Figure 4b. These results therefore suggest that crack tolerance occurs in electrospun fiber mats. Previous analytical modeling has indicated a relatively diffuse plastic zone in fibrous networks may exist,[16] which suggests a stress delocalization mechanism operates in our electrospun nanofibrous network samples. A mechanism to describe this delocalization must be based on the deformation behavior of individual electrospun nanofiber units within the network. Loading of the fibrous network in Figure 2 produces a relatively linear elastic deformation region where the individual nanofibers are expected to be elastically deforming along their length. Critically, the crack length provides little effect on this initial linear elastic region and indicates that the nanofibers will be deforming along their whole length. The deformation behavior will therefore depend on the volume of fibers being loaded in the network and not the number of fibers in the cross-sectional width of the sample as described by W in eq 1. The stress delocalization will originate from the fibers sharing the load in the network along their full length, much like wires in tension under loading. This mechanism is markedly different from continuum solids where load is increasingly carried around a crack tip causing stress localization. Additionally, interactions between fibers from contact points in network plays an important role in distributing and transferring stresses throughout the network.[17] Strong bonding between fibers can increase the toughness of a fibrous network.[42] However, the transfer of stresses in nonwoven fabrics is not well characterized as it takes place in knitted or braided composites. Recent work has shown how high polar interactions can occur between PA6 nanofibers,[30] and we suggest

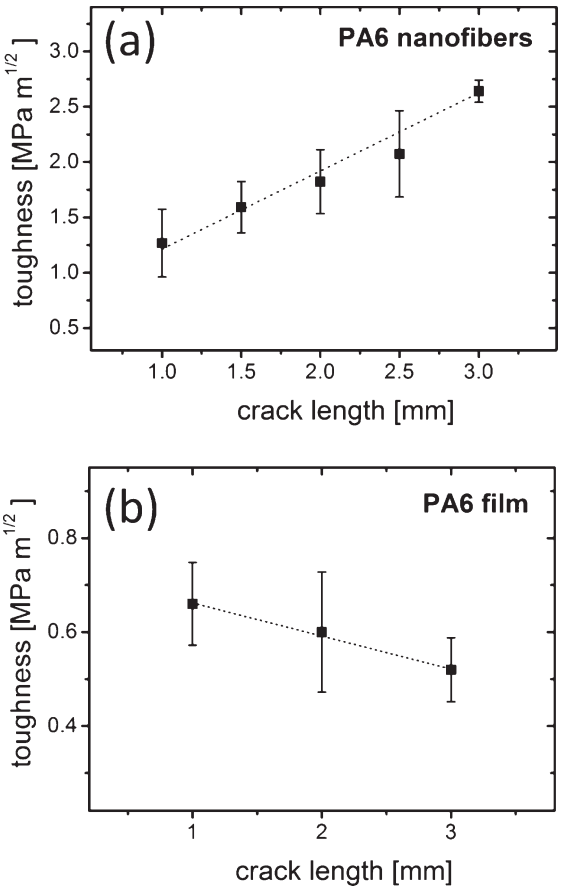

Figure 4. Plot of the fracture toughness of (a) an electrospun nanofiber network and (b) an cast polymer film against macroscopic size of a double notch incorporated into the samples.

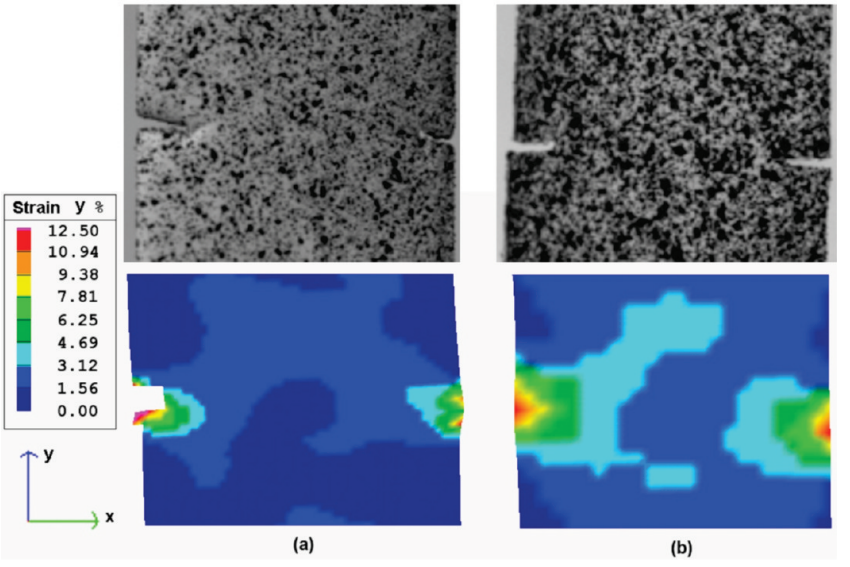

Figure 5. Image analysis of the strain distribution in (a) a notched electrospun nanofiber network and (b) a comparable notched polymer film, during tensile loading in the Y axis using a load of approximately 1 N and resultant sample strain of 12%.

that these interactions may provide effective stress transfer between nanofibers in nonwoven electrospun mats. The deformation behavior will therefore depend on the volume of fibers being loaded in the network and not the number of fibers in the cross-sectional width of the sample as described in eq 1.

To explore the concept of stress delocalization in the electrospun nanofibrous network, we map sample strain for a notched electrospun nanofiber network and comparable thin polymer during tensile testing using image analysis (see Methods section). Figure 5 displays the magnitude of strain, which is proportional to stress, spatially throughout both the fibrous network and polymer film. The 2D maps presented in Figure 5 are for the same 12% sample strain and stress from a 1 N load in both the fibrous network and film, allowing a direct comparison of the strain distribution between the two sample geometries to be made. The electrospun fibrous network in Figure 5a indicates a slight strain concentration at the notch tips but this strain does not radiate out toward the opposing crack, highlighting how a stress concentration between the notches is absent. However, strain mapping of a comparably notched polymer film shown in Figure 5b indicates an increase in the strain concentration around and between the notches. Thus, the image analysis supports our claims of stress delocalization mechanisms in the electrospun fibrous network as opposed to the classical description of stress concentration around crack tips as exhibited in the polymer film example. The stress delocalization around the crack tip in the electrospun fibrous network supports theoretical evaluations of networks that deform relatively homogeneously throughout their volume despite the incorporation of cracks with lengths significantly larger than the network fiber diameter.[14,15,38] This stress delocalization between notches in the electrospun PA6 nanofiber networks therefore provides sample tensile strength and elastic modulus, which is independent of crack length and reflected in an apparently increasing toughness using fracture mechanics evaluations.

CONCLUSIONS

In this study, the mechanical properties of electrospun PA6 nanofiber networks are examined. The fracture behavior of the electrospun fibrous networks was observed to be independent of crack length, included in the sample to induce failure, indicated an apparent increase in the fracture toughness with increasing crack length. This enhancement of toughness was attributed to stress delocalization in the fibrous network and is not accounted for in classical fracture toughness evaluations applied to continuum solids. Image analysis supported the stress delocalization mechanism in the fibrous network when compared to a comparable polymer film. This crack independent fracture behavior of the electrospun fiber network indicates how the material may have novel applications in areas such as protective clothing and packaging. In addition, the fibrous network structures found in natural systems, such as spider's web, will also be expected to display similar crack independent fracture behavior, thus facilitating integrity of the network despite potentially numerous damage zones being present.

AUTHOR INFORMATION

Corresponding Author

*E-mail: a.h.barber@qmul.ac.uk. Phone: +44 (0)20 7882 7763. Fax: +44 (0)20 7882 3390.

ACKNOWLEDGMENT

We thank Dr Zofia Luklinska at Queen Mary University of London, NanoVision Centre for assisting with microscopy facilities.

REFERENCES

(1) Fratzl, P.; Gupta, H. S.; Fischer, F. D.; Kolednik, O. *Adv. Mater.* **2007**, *19*, 2657–2661.
(2) Gupta, H. S.; Stachewicz, U.; Wagermaier, W.; Roschger, P.; Wagner, H. D.; Fratzl, P. *J. Mater. Res.* **2006**, *21*, 1913–1921.
(3) Calvert, P.; Cesarano, J.; Chandra, H.; Denham, H.; Kasichainula, S.; Vaidyanathan, R. *Philos. Trans. R. Soc. A* **2002**, *360*, 199–209.
(4) Barber, A. H.; Wiesel, E.; Wagner, H. D. *Compos. Sci. Technol.* **2002**, *62*, No. PII S0266-3538(02)00112-4.
(5) Argon, A. S.; Cohen, R. E. *Polymer* **2003**, *44*, 6013–6032.
(6) Cox, B. N. *J. Mater. Sci.* **1996**, *31*, 4871–4881.
(7) Vollrath, F.; Porter, D. *Polymer* **2009**, *50*, 5623–5632.
(8) Gosline, J. M.; Guerette, P. A.; Ortlepp, C. S.; Savage, K. N. *J. Exp. Biol.* **1999**, *202*, 3295–3303.
(9) Yang, Y.; Chen, X.; Shao, Z. Z.; Zhou, P.; Porter, D.; Knight, D. P.; Vollrath, F. *Adv. Mater.* **2005**, *17*, 84–88.
(10) Gosline, J. M.; Denny, M. W.; Demont, M. E. *Nature* **1984**, *309*, 551–552.
(11) Eichhorn, S. J.; Dufresne, A.; Aranguren, M.; Marcovich, N. E.; Capadona, J. R.; Rowan, S. J.; Weder, C.; Thielemans, W.; Roman, M.; Renneckar, S.; Gindl, W.; Veigel, S.; Keckes, J.; Yano, H.; Abe, K.; Nogi, M.; Nakagaito, A. N.; Mangalam, A.; Simonsen, J.; Benight, A. S.; Bismarck, A.; Berglund, L. A.; Peijs, T. *J. Mater. Sci.* **2010**, *45*, 1–33.
(12) Black, L. D.; Allen, P. G.; Morris, S. M.; Stone, P. J.; Suki, B. *Biophys. J.* **2008**, *94*, 1916–1929.
(13) Janmey, P. A.; Euteneuer, U.; Traub, P.; Schliwa, M. *J. Cell. Biol.* **1991**, *113*, 155–160.
(14) Hudson, N. E.; Houser, J. R.; O'Brien, E. T.; Taylor, R. M.; Superfine, R.; Lord, S. T.; Falvo, M. R. *Biophys. J.* **2010**, *98*, 1632–1640.
(15) Buell, S.; Rutledge, G. C.; Van Vliet, K. J. *ACS Appl. Mat. Inter.* **2010**, *2*, 1164–1172.
(16) Isaksson, P. *Eng. Fract. Mech.* **2010**, *77*, 1240–1252.
(17) Bobaru, F. *Model. Simul. Mater. Sc.* **2007**, *15*, 397–417.
(18) Reneker, D. H.; Chun, I. *Nanotechnology* **1996**, *7*, 216–223.
(19) Fridrikh, S. V.; Yu, J. H.; Brenner, M. P.; Rutledge, G. C. *Phys. Rev. Lett.* **2003**, *90*, 144502.
(20) Eichhorn, S. J.; Sampson, W. W. *J. R. Soc., Interface* **2009**, *7*, 641–649.
(21) Bognitzki, M.; Czado, W.; Frese, T.; Schaper, A.; Hellwig, M.; Steinhart, M.; Greiner, A.; Wendorff, J. H. *Adv. Mater.* **2001**, *13*, 70–72.
(22) Carnell, L. S.; Siochi, E. J.; Holloway, N. M.; Stephens, R. M.; Rhim, C.; Niklason, L. E.; Clark, R. L. *Macromolecules* **2008**, *41*, 5345–5349.
(23) Kearney, A. V.; Litteken, C. S.; Mohler, C. E.; Mills, M. E.; Dauskardt, R. H. *Acta Mater.* **2008**, *56*, 5946–5953.
(24) Burman, M.; Arinstein, A.; Zussman, E. *Appl. Phys. Lett.* **2008**, *93*, 193118.
(25) Wang, W.; Bushby, A. J.; Barber, A. H. *Appl. Phys. Lett.* **2008**, *93*, 201907.
(26) Wang, W.; Peijs, T.; Barber, A. H. *Nanotechnology* **2010**, *21*, 035705.
(27) Gu, S. Y.; Wu, Q. L.; Ren, J.; Vancso, G. J. *Macromol. Rapid Commun.* **2005**, *26*, 716–720.
(28) Zussman, E.; Burman, M.; Yarin, A. L.; Khalfin, R.; Cohen, Y. *J. Polym. Sci., Part B: Polym. Phys.* **2006**, *44*, 1482–1489.
(29) Arinstein, A.; Burman, M.; Gendelman, O.; Zussman, E. *Nat. Nanotechnol.* **2007**, *2*, 59–62.
(30) Stachewicz, U.; Barber, A. H. *Langmuir* **2011**, *27*, 3024–3029.
(31) Ifkovits, J. L.; Devlin, J. J.; Eng, G.; Martens, T. P.; Vunjak-Novakovic, G.; Burdick, J. A. *ACS Appl. Mater. Interfaces* **2009**, *1*, 1878–1886.

(32) Hohman, M. M.; Shin, M.; Rutledge, G.; Brenner, M. P. *Phys. Fluids* **2001**, *13*, 2201–2220.
(33) Carrizales, C.; Pelfrey, S.; Rincon, R.; Eubanks, T. M.; Kuang, A. X.; McClure, M. J.; Bowlin, G. L.; Macossay, J. *Polym. Adv. Technol.* **2008**, *19*, 124–130.
(34) Li, X. H.; Ding, B.; Lin, J. Y.; Yu, J. Y.; Sun, G. *J. Phys. Chem. C* **2009**, *113*, 20452–20457.
(35) Bazbouz, M. B.; Stylios, G. K. *J. Polym. Sci., Polym. Phys.* **2010**, *48*, 1719–1731.
(36) Hang, F.; Dun, L.; Bailey, R.; Jimenez-Palomar, I.; Stachewicz, U.; Cortes-Ballesteros, B.; Davies, M.; Zech, M.; Bödefeld, C.; Barber, A. H. Unpublished work.
(37) Wu, X. F.; Dzenis, Y. A. *J. Phys. D Appl. Phys.* **2007**, *40*, 4276–4280.
(38) Huisman, E. M.; Heussinger, C.; Storm, C.; Barkema, G. T. *Phys. Rev. Lett.* **2010**, *105*, 118101.
(39) Klemann, B. M.; DeVilbiss, T. *Polym. Eng. Sci.* **1996**, *36*, 126–134.
(40) Knott, J. K. *Fundamentals of Fracture Mechanics*; Butterworth & Co.: London, 1973; p 63.
(41) Sobieraj, M. C.; Kurtz, S. M.; Rimnac, C. M. *Biomaterials* **2005**, *26*, 3411–3426.
(42) Raisanen, V. I.; Alava, M. J.; Nieminen, R. M. *J. Appl. Phys.* **1997**, *82*, 3747–3753.